FULL PAPER

Dalton
www.rsc.org/dalton

Self-assembly of tetranuclear $\{[Co(trien)]_2[W(CN)_8]_2\}^{2-}$ or $\{[Co(tren)]_2[W(CN)_8]_2\}^{2-}$ squares with alternating aliphatic tetramine Co(III) and octacyanotungstate(IV) corners †

Rafał Kania, Krzysztof Lewiński and Barbara Sieklucka *
Faculty of Chemistry, Jagiellonian University, Ingardena 3, 30-060 Krakow, Poland.
E-mail: siekluck@chemia.uj.edu.pl

Received 29th October 2002, Accepted 2nd January 2003
First published as an Advance Article on the web 3rd February 2003

The self-assembly of $[W(CN)_8]^{4-}$ with *cis*-$[Co^{III}(N_4)Cl(OH_2)]^{2+}$ {N_4 = trien = triethylenetetraamine and tren = tris(2-aminoethylene)amine} in aqueous solution generates supramolecular assemblies: $K_2[Co^{III}(trien)]_2[W^{IV}(CN)_8]_2\cdot 8H_2O\cdot EtOH$ (**1**) and $K_2[Co^{III}(tren)]_2[W^{IV}(CN)_8]_2\cdot 9H_2O$ (**2**). The crystal structure of **2** has been determined. The Co(III) and W(IV) centres linked alternatively by single cyano bridge afford $\{[Co(tren)]_2[W(CN)_8]_2\}^{2-}$ square units joined by potassium ions into the bilayer structure. The products exhibit metal-to-metal charge-transfer (MMCT) transitions at 519 nm (**1**) and 512 nm (**2**) in aqueous solution. The self-assembly of $[W(CN)_8]^{4-}$ and *cis*-$[Co^{III}(trien)Cl(OH_2)]^{2+}$ into the tetranuclear square $\{[Co(trien)]_2[W(CN)_8]_2\}^{2-}$ proceeds by two parallel reaction pathways with the rate law $d\{[Co(N_4)]_2[W(CN)_8]\}/dt = k_a[Co(N_4)]^2[W(CN)_8] + k_b[Co(N_4)][W(CN)_8] + k_{-b}[Co(N_4)]$ where $k_a = 4.89 \times 10^2$ dm^6 mol^{-2} s^{-1}, $\Delta H^{\neq} = 46$ kJ mol^{-1}, $\Delta S^{\neq} = -38$ J K^{-1} mol^{-1}; $k_b = 2.14 \times 10^{-1}$ dm^3 mol^{-1} s^{-1}, $\Delta H^{\neq} = 121$ kJ mol^{-1}, $\Delta S^{\neq} = +149$ J K^{-1} mol^{-1}; $k_{-b} = 0.66 \times 10^{-3}$ dm^3 mol^{-1} s^{-1}, $\Delta H^{\neq} = 68$ kJ mol^{-1}, $\Delta S^{\neq} = -77$ J K^{-1} mol^{-1} ($T = 25$ °C, pH = 2 (HCl + KCl), $I = 0.5$ mol dm^{-3}). The k_a pathway corresponds to the ion-triplet $\{Co^{III},W^{IV},Co^{III}\}$ formation followed by rate-determining outer-sphere electron transfer, subsequent fast substitution by $[W(CN)_8]^{4-}$ and spontaneous back electron transfer to give $Co_2^{III}W_2^{IV}$, whereas the k_b pathway is consistent with the rate-determining reversible cyano bridged dimer formation within an ion-pair $\{Co^{III},W^{IV}\}$ followed by inner-sphere electron transfer, fast aggregation and spontaneous back electron transfer to give the final $Co_2^{III}W_2^{IV}$ product.

Introduction

The crystal engineering of cyano bridged supramolecular coordination architectures based on octacyanometallate(IV,V) (M = Mo and W) molecular building blocks is currently an area of extensive research. The driving force for the research in this field is the generation, by deliberate design, of functional molecular networks with predetermined structures and potential for technologically useful molecule-based electronic, magnetic and photomagnetic applications.

The self-assembly strategies for the formation of supramolecular assemblies employing $[M(CN)_8]^{n-}$ and cationic 3d metal complexes with labile coordination sites are very limited.[1] In the metal-directed self-assembly of molecular squares, cubes and isolated molecules *cis*-protected octahedral complexes of transition metals have been employed.[1a,b,f,k] We have successfully used this strategy to synthesise hexanuclear cluster $\{[Mn(bpy)_2]_4[M(CN)_6]_2\}\cdot 14H_2O$ (M = Mo, W)[1b] and pentanuclear high-spin molecule $[Mn(bpy)_2][Mn(bpy)_2(H_2O)]_2[W(CN)_6]_2\cdot 7H_2O$[1k] based on *cis*-$[Mn(bpy)_2(H_2O)_2]^{2+}$.

In spite of a few synthetic strategies of the self-assembly processes, no attempts have been made to postulate a mechanistic pathway. The gaining of knowledge on the mechanism of the self-assembly process from octacyanometallates and cationic metal centres is of crucial importance in the rational development of new strategies for the crystal engineering of their coordination networks.

In an effort to extend the discrete cluster chemistry based on octacyanometallates, we have employed two isomeric *cis*-$[Co^{III}(N_4)Cl_2]^+$ (N_4 = aliphatic tetramine) complexes: *cis*-α-$[Co(trien)Cl_2]^+$ (trien = triethylenetetramine) and *cis*-$[Co(tren)Cl_2]^+$ (tren = tris(2-aminoethyl)amine) for the self-assembly with $[W(CN)_8]^{4-}$. The synthetic strategy is relying on the formation of Co–NC–W linkage *via* substitution of labile ligands by nitrogen end of cyanide. The tetradentate aliphatic tetramine ligand blocks four coordination sites on pseudo-octahedral Co(III) centre, preventing growth of the infinite polymeric structure.

Here, we report the synthesis and characterisation of tetranuclear $\{[Co(tren)]_2[W(CN)_8]_2\}^{2-}$ square units bridged by potassium ions into a 2D bi-layer $K_2\{[Co^{III}(tren)]_2[W^{IV}(CN)_8]_2\}\cdot 9H_2O$ array of MMCT characteristics. In order to understand the mechanism of the self-assembly of the tetranuclear square, we have studied the kinetics of the reaction of *cis*-$[Co(trien)Cl_2]^+$ with $[W(CN)_8]^{4-}$ in aqueous solution.

Experimental

All the chemicals used in the present study were purchased from Aldrich and used as received. The *cis*-α-$[Co(trien)Cl_2]Cl$[2,3] (hereafter named *cis*-$[Co(trien)Cl_2]Cl$) and $K_4[W(CN)_8]\cdot 2H_2O$[4] were prepared by the reported procedures. The elemental analyses of the compounds were consistent with their formulas. The $[Co(tren)Cl_2]Cl$ was obtained by the modified literature procedure.[5] A 9 ml portion of 30% H_2O_2 in 40 ml of water was added slowly with constant stirring to an ice-cold solution of 9.5 g (40 mmol) of $CoCl_2\cdot 6H_2O$ and 6 ml of tren (45 mmol) in 150 ml of H_2O. Then 50 ml of 3 M HCl was added to the solution. The final solution was evaporated on a steam bath until the product started to precipitate. The solution was cooled down in ice bath. Dark violet crystals were filtered off and washed in a small amount of cold water and ethanol. The purity of compound was checked by microanalysis. Anal. Calcd. for $[Co(C_6H_{18}N_4)Cl_2]Cl\cdot H_2O$: C, 21.87; N, 17.00; H, 6.12. Found: C, 21.86; N, 16.66; H, 6.07.

Synthesis of $K_2[Co^{III}(trien)]_2[W^{IV}(CN)_8]_2\cdot 8H_2O\cdot EtOH$ (1)

The equilibrated aqueous solution of *cis*-α-$[Co(trien)Cl(OH_2)]Cl$ was prepared by dissolving the solid *cis*-α-$[Co(trien)Cl_2]Cl$

† Electronic supplementary information (ESI) available: the distances (Å) and angles (°) of possible hydrogen bonds for $K_2\{[Co^{III}(tren)]_2[W^{IV}(CN)_8]_2\}\cdot 9H_2O$ (**2**); rate constants and activation parameters for the reaction of *cis*-α-$[Cr(trien)Cl(OH_2)]^{2+}$ with $[W(CN)_8]^{4-}$ in aqueous solution. See http://www.rsc.org/suppdata/dt/b2/b210669h/

DOI: 10.1039/b210669h

(124 mg, 0.4 mmol, 10 ml) in water and left until the aquation of the first Cl^- ligand was complete. Then it was mixed with $K_4[W(CN)_8]\cdot 2H_2O$ (234 mg, 0.4 mmol, 10 ml) aqueous solution. The resulting deep red solution was left for two hours for the completion of reaction. Then, ethanol was added drop-wise to the solution until the red–purple oil has appeared as the separate layer. The crude oil was purified by dissolving in small amount of water and subsequent addition of ethanol. The purifying procedure was repeated five times and finally the red–purple oil was solidified by the addition of acetone. The solid product was collected by suction filtration and dried in a desiccator over silica gel. All attempts to obtain single crystals were unsuccessful. Anal. Calcd. for $K_2\{[Co^{III}(C_6H_{18}N_4)]_2[W^{IV}(CN)_8]_2\}\cdot 8H_2O\cdot EtOH$: C, 24.63; N, 22.98; H, 4.00. Found: C, 24.55; N, 23.02; H, 4.03.

Synthesis of $K_2[Co^{III}(tren)]_2[W^{IV}(CN)_8]_2\cdot 9H_2O$ (2)

An equimolar aqueous solutions of $[Co(tren)Cl_2]Cl$ (124 mg, 0.4 mmol, 30 ml) and $K_4[W(CN)_8]\cdot 2H_2O$ (234 mg, 0.4 mmol, 30 ml) were mixed together. The solution became deep red and brown solid started to precipitate after a few minutes. After two hours the reaction mixture was separated into brown solid and filtrate. The solid was washed with distilled water and ethanol and air dried. Microanalysis: Calcd. for $K_2[Co^{III}(C_6H_{18}N_4)]_2[W^{IV}(CN)_8]_2\cdot 9H_2O$: C, 23.44; N, 23.43; H, 3.79. Found: C, 23.55; N, 23.40; H, 3.66. The filtrate was used to grow single crystals. Single crystals of $K_2\{[Co^{III}(tren)]_2[W^{IV}(CN)_8]_2\}\cdot 9H_2O$ were grown by slow diffusion of EtOH vapour into the filtrate. After one month the deep brown crystals were collected and washed with EtOH and air-dried. The composition of single crystals has been established by X-ray crystallography. The compound is sparingly soluble in water and polar organic solvents.

Kinetic measurements

Kinetics measurements were performed by using conventional mixing technique in the tandem quartz cells. The kinetics of the aggregation reaction of *cis*-$[Co(trien)Cl(OH_2)]^{2+}$ with $[W(CN)_8]^{4-}$ were measured on a Shimadzu 2101 PC spectrophotometer equipped with a thermoelectrically controlled cell holder CPS 60. The progress of the reaction was monitored by following the change of absorbance at 550 nm. All the measurements were carried out under pseudo-conditions with the excess of $[W(CN)_8]^{4-}$ over the *cis*-$[Co(trien)Cl(OH_2)]^{2+}$ complex. The rate constants were determined from the average of two or three replicate experiments. The reaction temperature was maintained to within 0.1 °C over the range 10–30 °C. The ionic strength I of the reaction solutions was maintained at 0.5 mol dm^3 with added potassium chloride, and the pH of the solutions was controlled in the pH range 2–9 using universal buffer solutions consisting of phosphoric, acetic and boric acid and KOH.[6] The rate constants were obtained by numerical fitting of appropriate kinetic curves. Calculations were performed by the application of the kinetics-modelling procedure included in the Specfit® software package.[7] The stock solutions of the *cis*-$[Co(trien)Cl(OH_2)]^{2+}$ ion were prepared by dissolving the solid *cis*-$[Co(trien)Cl_2]Cl$ in the appropriate aqueous buffered solutions and left overnight until the aquation of the first Cl^- ligand was complete. The stock solutions were controlled before each series of kinetics measurement by means of UV-VIS spectra.[3a,b]

Physical measurements

UV-visible spectra were measured on a Shimadzu 2101 PC spectrophotometer. The overall equilibrium constant β of the reaction of *cis*-$[Co(trien)Cl(OH_2)]^{2+}$ with $[W(CN)_8]^{4-}$ and molar absorbance coefficient (ε_{max}) of the $\{[Co^{III}(trien)]_2[W^{IV}(CN)_8]_2\}^{2-}$ product were determined from the set of spectra by the Job method. The calculations were performed by using a least squares fitting routine included in the Specfit software package.[7] The IR spectra were measured on a Bruker model FT-IFS 47 spectrometer in KBr pellets. The cyclic voltammetry measurements were performed with multipurpose electrochemical analyser EA9 (MTM). A standard three-electrode configuration with Pt working and counter electrode and Ag/AgCl reference electrode was used. Mass spectra measurements were performed with Electrospray Ionisation Mass Spectrometer (ESMS) Finnigan MAT 95S double focusing instrument with reversed geometry, BE (B = magnetic field and E = electric field). Spectra were taken in a positive ion mode using magnetic scan over the m/z range from 250 to 2000. The scan speed was set to 5 s $decade^{-1}$ and standard settings of cone voltage and the lenses were as follows: cone voltage 2.5 kV; heated capillary −10 V; skimmer −1.5 V and octapole −4 V. The source was optimised on the double charged peak of gramicidin S at m/z of 571.3. The sample was dissolved in a mobile phase consisted of 30% MeOH in water supplemented with 0.1% formic acid. The flow rate was maintained at 30 µl min^{-1} and samples were injected *via* a Rheodyne injector equipped with a 5 µl loop.

Crystallography

The X-ray diffraction data were collected at room temperature on a Nonius Kappa CCD diffractometer using Mo-Kα radiation (λ = 0.7107 Å). The diffraction pattern for all tested crystals showed that they are non-merohedral twins. For data collection we have chosen the speciment of size 0.2 × 0.2 × 0.1 mm that showed the smallest contribution from additional diffraction pattern. The Denzo-Scalepack[8] program package was used for cell refinement and data reduction. A multi-scan absorption correction based on equivalent reflections was applied to the data. The structure was solved by the Patterson method (SHELXS-97)[9] and subsequent Fourier analyses. Anisotropic displacement parameters were applied to non-hydrogen atoms in full-matrix least-squares refinement based on F^2 using (SHELXL-97).[9] The hydrogen atoms of tren molecules were located in their calculated positions and refined using a riding model with isotropic displacement factors. Water hydrogens were not included in the refinement. The highest peak on difference Fourier map is located 1 Å from W2 atom. Crystal data for **2**: $C_{28}H_{54}N_{24}O_9Co_2K_2W_2$, M = 1434.72, triclinic, space group $P\bar{1}$, Z = 2, a = 11.7830(2) Å, b = 13.0640(2) Å, c = 16.4650(2) Å, α = 84.770(1)°, β = 83.429(1)°, γ = 88.595(1)°, V = 2507.1(1) $Å^3$, μ = 5.460 mm^{-1}. The final factors R_1 = 0.0978 and wR_2 = 0.2612 have high values due to twinning, however the quality of the structure is adequate to allow comparison of metal–ligand bond lengths and angles.

CCDC reference number 196411.

See http://www.rsc.org/suppdata/dt/b2/b210669h/ for crystallographic data in CIF or other electronic format.

Results and discussion

Crystal structure of $K_2\{[Co^{III}(tren)]_2[W^{IV}(CN)_8]_2\}\cdot 9H_2O$

The crystal structure of $K_2\{[Co^{III}(tren)]_2[W^{IV}(CN)_8]_2\}\cdot 9H_2O$ consists of tetranuclear $\{[Co^{III}(tren)]_2[W^{IV}(CN)_8]_2\}^{2-}$ square units, potassium ions and H_2O molecules. The symmetrically independent part of the structure with the atom labelling scheme is given in Fig. 1 and the selected bond lengths and angles are listed in Table 1. The tetranuclear unit consists of alternating $[Co^{III}(tren)]$ and $[W^{IV}(CN)_8]$ corners. The diagonal dimensions of the tetramer are 7.92 and 6.63 Å for the W1–W2 and Co1–Co2 diagonals, respectively. Each W atom has eight cyano ligands arranged in a slightly distorted square antiprismatic geometry (D_{4d}). Four of the W(1) and three of the W(2) ligands form cyano-bridges between W, Co and K ions. Within experimental error, there are no dimensional differences

Table 1 Selected bond lengths (Å) and angles (°) for $K_2\{[Co^{III}(tren)]_2[W^{IV}(CN)_8]_2\}\cdot 9H_2O$ (**2**)[a]

W(1)–C(11)	2.128(12)	W(2)–C(21)	2.163(14)
W(1)–C(12)	2.144(16)	W(2)–C(22)	2.130(13)
W(1)–C(13)	2.161(14)	W(2)–C(23)	2.132(15)
W(1)–C(14)	2.134(16)	W(2)–C(24)	2.102(16)
W(1)–C(15)	2.170(15)	W(2)–C(25)	2.176(15)
W(1)–C(16)	2.140(15)	W(2)–C(26)	2.139(15)
W(1)–C(17)	2.184(15)	W(2)–C(27)	2.175(15)
W(1)–C(18)	2.150(14)	W(2)–C(28)	2.174(16)
C(11)–W(1)–C(18)	72.9(5)	C(21)–W(2)–C(22)	73.3(5)
C(16)–W(1)–C(17)	72.7(7)	C(26)–W(2)–C(28)	70.7(7)
C(17)–W(1)–C(18)	73.9(6)	C(21)–W(2)–C(28)	73.3(6)
C(11)–W(1)–C(16)	143.6(6)	C(22)–W(2)–C(26)	144.1(7)
Co(1)–N(18)	1.896(12)	Co(2)–N(11)	1.905(10)
Co(1)–N(22)	1.919(12)	Co(2)–N(21)	1.904(11)
Co(1)–N(30)	1.934(13)	Co(2)–N(40)	1.955(12)
Co(1)–N(31)	1.934(10)	Co(2)–N(41)	1.939(10)
Co(1)–N(34)	1.953(12)	Co(2)–N(44)	1.955(14)
Co(1)–N(37)	1.965(13)	Co(2)–N(47)	1.953(14)
N(18)–Co(1)–N(22)	90.6(5)	N(11)–Co(2)–N(21)	91.4(5)
K(1)–O(1)	2.76(2)	K(2)–O(3)	2.77(2)
K(1)–O(2)	2.76(2)	K(2)–O(5)	2.83(2)
K(1)–O(3)	2.68(2)	K(2)–O(7)	2.81(2)
K(1)–O(4)	3.17(2)	K(2)–O(6)	3.09(2)
K(1)–N(26)	3.18(2)	K(2)–N(28)	2.93(2)
K(1)–N(16)#1	2.82(2)	K(2)–N(12)#2	3.34(2)
K(1)–N(15)#2	2.94(2)	K(2)–N(17)#3	2.79(2)
O(3)–K(1)–N(26)	67.3(7)	O(3)–K(2)–N(28)	67.5(7)
O(3)–K(1)–N(16)#1	149.2(8)	O(3)–K(2)–N(17)#3	129.4(8)
N(16)#1–K(1)–N(26)	137.9(7)	N(17)#3–K(2)–N(28)	141.5(8)

[a] Symmetry operations used to generate equivalent atoms — #1: $x, y-1, z+1$; #2: $-x, -y+1, -x+1$; #3: $x, y, z+1$.

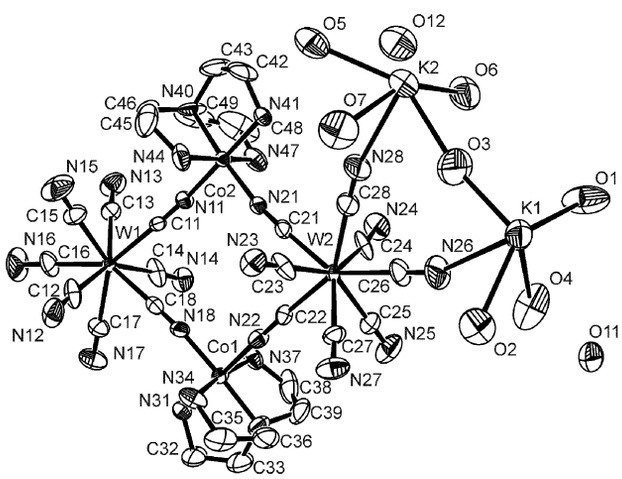

Fig. 1 An ORTEP[10] drawing of the asymmetric unit of the crystal structure of $K_2\{[Co^{III}(tren)]_2[W^{IV}(CN)_8]_2\}\cdot 9H_2O$.

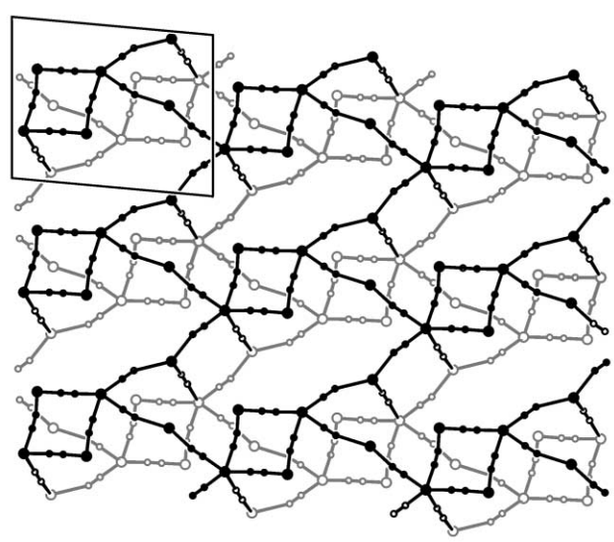

Fig. 2 An ORTEP[10] drawing along [100] direction of the layer topology of $K_2\{[Co^{III}(tren)]_2[W^{IV}(CN)_8]_2\}\cdot 9H_2O$. Only the bridging cyano groups are shown for clarity. The upper layer is black, the bottom layer is grey.

between the mean values for the bridging and terminal cyano ligands. The W–C and C–N bond distances of 2.15(2) and 1.15(2) Å, respectively, are in range of typical for other, isolated and bridging, octacyanotungstates(IV).[1b,d,g,j–l,11] The bridging CN ligands exhibit almost linear W–C–N units (maximum deviation from linearity of 5°) and slightly bent Co–N–C units with the angles ranging from 166(1) to 173(1)°. The hexa-coordinate Co atoms present a distorted octahedral geometry. The bond lengths and angles in the $[Co(tren)]^{2+}$ unit are typical for polyamine Co^{III} complexes.[12] Two *cis* positions in $[Co(tren)(NC)_2]^+$ moiety are occupied by the nitrogen atoms of the cyanide bridging groups with the average distance Co–N (CN) of 1.91(1) Å. The square $\{[Co(tren)]_2[W(CN)_8]_2\}^{2-}$ units connected by potassium ions coordinating cyano groups form two-dimensional layers parallel to the (100) plane (Fig. 2). The coordination spheres of both potassium ions are significantly different. The K(1) ion is seven coordinate with four water molecules and three cyano ligands while the K(2) ion is coordinated by four water molecules and two cyano ligands. The higher than usually observed coordination number of K(1) forces N(26) and O(4) atoms to be at distances 3.18 and 3.17 Å respectively, longer than for other donor atoms. Also, in the K(2) coordination sphere the distance to water O(6) is 3.09 Å, longer than typical. The average distance for the other K–N is 2.87(7) Å, C–N–K angles are in the range from 148 to 164°, and are comparable to those found for other cyano bridged

potassium ions,[13,14] while the average distance for other waters is 2.77(5) Å. The water molecule O(3) bridges both potassium ions. An additional two crystalline water molecules are not coordinated by any metal ion. The given layer and neighboring layer related by $(-x, -y + 1, -z + 1)$ symmetry are linked in pairs by cyano group CN(15) coordinating to potassium K(1). That results in formation of bilayers connected by centrosymmetric square units made of K(1) and W(1) bridged by cyanide groups (Fig. 3). Layers are also linked by hydrogen bonds between NH_2 groups of the tris(2-aminoethylene)amine ligand and terminal cyano groups with distances between donor and acceptor in the 2.903–3.074 Å range. The hydrogen atoms of water molecules were not determined, however distances from oxygen atoms to cyanide nitrogens and other oxygens indicate that, except for bridging O3, all molecules of water are involved in the formation of a hydrogen bond network. Distances between donor and acceptor are in the range of 2.724–3.050 Å. Details of hydrogen bond geometries are available as ESI (Table S1). † Water molecules O11 and O12 positioned between bi-layers contribute to formation of hydrogen bonds that link bi-layers together and are different from those observed within bi-layers. We conclude that the crystal structure should be considered as build from bi-layers rather than single layers.

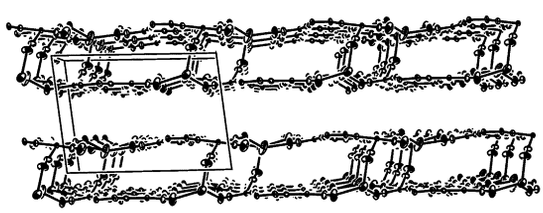

Fig. 3 A view of the layer arrangement in the structure of **2**. The water molecules were omitted for clarity. The view is along the [010] direction.

Electrospray ionisation mass spectrum of $K_2[Co^{III}(trien)]_2[W^{IV}(CN)_8]_2\cdot 8H_2O\cdot EtOH$ (1)

The ESI MS mass spectrum of **1** in aqueous solution (Fig. 4) shows major peaks at *m*/*z* 675.2 and 1310.8 that can be assigned to pseudomolecular doubly charged $\{2K^+ + K_2[Co^{III}(trien)]_2[W^{IV}(CN)_8]_2\}^{2+}$ and singly charged $\{K^+ + K_2[Co^{III}(trien)]_2[W^{IV}(CN)_8]_2\}^+$ ions and a signal at *m*/*z* 586.9 that can be attributed to the singly charged $\{K^+ + K_4[W(CN)_8]\}^+$ ion. The two bands at *m*/*z* 948.5 and 993.4 can be assigned to a multicharged clusters $\{2K^+ + 2(K_2[Co^{III}(trien)]_2[W^{IV}(CN)_8]_2) + K_4[W(CN)_8]\}^{2+}$ and $\{4K^+ + 3(K_2[Co^{III}(trien)]_2[W^{IV}(CN)_8]_2)\}^{4+}$. All peaks connected with the product feature the isotopic pattern of tungsten natural isotopic pattern (^{180}W 0.12%, ^{182}W 26.49%, ^{183}W 14.30%, ^{184}W 30.64%, ^{186}W 28.42%). The ESI MS of **1** strongly suggests that $K_2[Co^{III}(trien)]_2[W^{IV}(CN)_8]_2\cdot 8H_2O\cdot$ EtOH dissolved in water contains the $\{[Co^{III}(trien)]_2[W^{IV}(CN)_8]_2\}^{2-}$ building unit. The integrity of the $\{[Co^{III}(trien)]_2[W^{IV}(CN)_8]_2\}^{2-}$ complex ion is retained in large part in the positive ion ESI MS at low cone voltage.

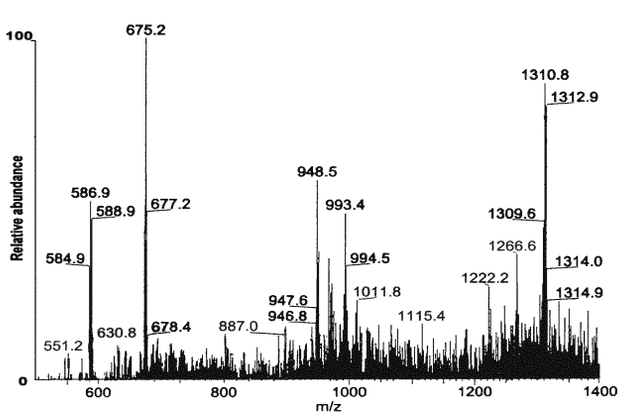

Fig. 4 The electrospray mass spectrum of $\{[Co^{III}(trien)]_2[W^{IV}(CN)_8]_2\}^{2-}$ (**1**).

Electrochemistry

The cyclic voltammograms of $K_2[Co^{III}(trien)]_2[W^{IV}(CN)_8]_2\cdot 8H_2O\cdot EtOH$ (**1**) and $K_2[Co^{III}(tren)]_2[W^{IV}(CN)_8]_2\cdot 9H_2O$ (**2**) recorded in aqueous solution (0.1 M KCl) are shown in Fig. 5. In both systems two W(IV)-centred one-electron oxidation waves *versus* Ag/AgCl electrode are observed. The first oxidation is reversible [$E^1_{1/2} = 0.33$ V, $\Delta E_p = 56$ mV, $i_{pa} \approx i_{pc}$ for **1** and $E^1_{1/2} = 0.35$ V, $\Delta E_p = 54$ mV, $i_{pa} \approx i_{pc}$ for **2**]. The second oxidation is quasi-reversible [$E^2_{1/2} = 0.67$ V, $\Delta E_p = 120$ mV, $i_{pa} \approx i_{pc}$ for **1** and $E^2_{1/2} = 0.68$ V, $\Delta E_p = 110$ mV, $i_{pa} \approx i_{pc}$ for **2** over scan rate 10–250 mV s^{-1}]. Cyclic voltammetry on $\{[Co^{III}(N_4)]_2[W^{IV}(CN)_8]_2\}^{2-}$ systems identifies two one-electron $[W(CN)_8]^{3-/4-}$ redox processes and representing stepwise oxidation of the two W^{IV} centres. The observed splitting of redox waves conforms to the analogue phenomenon in symmetrical bridged binuclear and trinuclear cyano-bridged complexes.[15–17] The separation by $\Delta E_{1/2}$(**1**,**2**) ≈ 0.34 V between the two oxidants shows strong electronic coupling of W sites. The broadening of the second wave shows the influence of bound Co^{III} centre on the $[W^{IV}(CN)_8]^{4-/3-}$ redox couple. The bridging unit –CN–Co^{III}(L)–NC– is revealed to be efficient linkage for W sites interaction due to the dπ(M)–pπ(CN) bonding system.[18] Moreover, an additional irreversible reduction wave observed at 0.51 V for **1** and **2** is due to reduction of Co^{III} site. Reversibility of the $Co^{III/II}$ couples is dependent on the electrode used and the nature of the blocking ligand.[15] The isolated $[Co^{III/II}(N_4)Cl_2]^+$ couples show irreversibility ($E_{1/2} = -0.51$ V *vs.* Ag/AgCl at Pt-electrode in DMSO with 0.2M $Bu_4N\cdot PF_6$) with complete loss of anodic wave at a scan rate up to 200 mV s^{-1}.

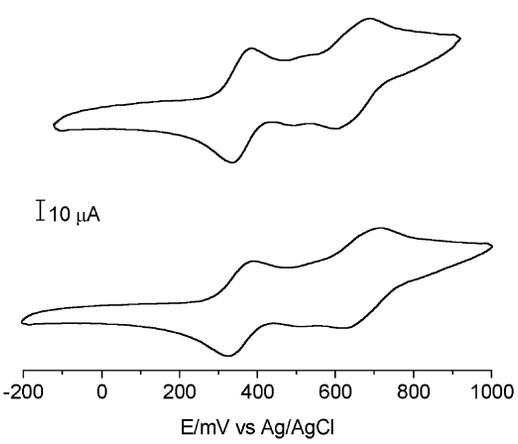

Fig. 5 The cyclic voltammograms of $K_2\{[Co^{III}(tren)]_2[W^{IV}(CN)_8]_2\}$ (top) and $K_2\{[Co^{III}(trien)]_2[W^{IV}(CN)_8]_2\}$ (bottom) in 0.1 mol dm^{-3} KCl.

Spectroscopic characterisation

The visible aqueous solution electronic spectra of $K_2[Co^{III}(trien)]_2[W^{IV}(CN)_8]_2\cdot 8H_2O\cdot EtOH$ (**1**) and $K_2[Co^{III}(tren)]_2[W^{IV}(CN)_8]_2\cdot 9H_2O$ (**2**) featuring three bands are presented in Fig. 6. Spectral deconvolution analysis of the $\{[Co^{III}(trien)]_2[W^{IV}(CN)_8]_2\}^{2-}$ spectrum shows the presence of four bands. The lowest energy bands at 519 nm (**1**) and 512 nm (**2**) are assigned to the $W^{IV} \longrightarrow Co^{III}$ MMCT transition. The band at 430 nm of $[Co^{III}(N_4)]_2[W^{IV}(CN)_8]_2^{2-}$ may be accounted for by the superposition of LF bands characteristic of $[W(CN)_8]^{4-}$ [1g] and $[Co^{III}(N_4)(NC)_2]^+$ [15,19,20] moieties. The band at 355 nm can be ascribed to the superposition of LF and MLCT transitions of $[W(CN)_8]^{4-}$ and $[W(CN)_8]^{3-}$,[21] respectively, and finally the 307 nm band is characteristic of MLCT transition of $[W(CN)_8]^{3-}$.[21,22c] LF bands of $[Co^{II}(N_4)(NC)_2]$ have been not

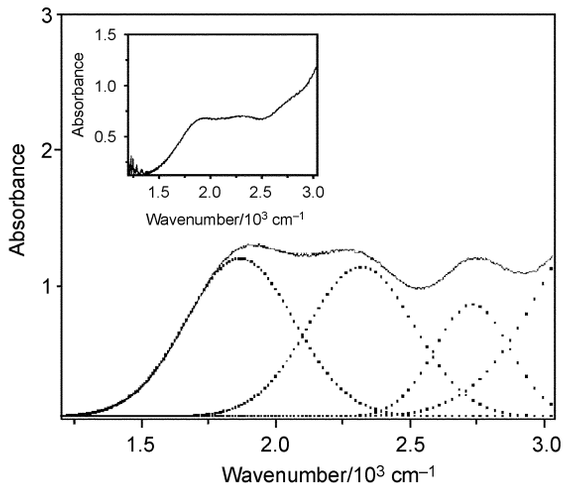

Fig. 6 The electronic spectra of aqueous solutions of $\{[Co^{III}(trien)]_2[W^{IV}(CN)_8]_2\}^{2-}$ (c_{tot} = 5.4 × 10^{-4} mol dm^{-3}) and its spectral deconvolution. Inset: the electronic spectra of aqueous solutions of $\{[Co^{III}(tren)]_2[W^{IV}(CN)_8]_2\}^{2-}$ (c_{tot} = 4.4 × 10^{-4} mol dm^{-3}).

included into the deconvolution procedure because of their very low intensities.[23] The presence of W^{V} band suggests small charge delocalisation between W^{IV} and Co^{III} centres resulting in the existence of electronic isomers $\{[Co^{III}(N_4)]_2[W^{IV}(CN)_8]_2\}^{2-}$ and $\{[Co^{II}(N_4)]_2[W^{V}(CN)_8]_2\}^{2-}$.[22] Small shifts in the band energies and changes in the intensities of the bands compared to the isolated $[W(CN)_8]^{4-}$ and $[W(CN)_8]^{3-}$ ions can be attributed to the effect of coordination of W–CN to Co^{III} centre, resulting in the decrease of their symmetry, and charge delocalisation. This conforms to the spectroscopic characterisation of mixed-valence $\{[Pt^{IV}L_4][Mo^{IV}(CN)_8]_2\}^{4-}$ system.[1g] The oxidation of $\{[Co^{III}(trien)]_2[W^{IV}(CN)_8]_2\}^{2-}$ to $\{[Co^{III}(trien)]_2[W^{V}(CN)_8]_2\}^{-}$ with $S_2O_8^{2-}$ [15] (Fig. 7) leading to an increase in the intensity of the 355 nm band (MLCT of $[W(CN)_8]^{3-}$)[1g] and a decrease in the intensity of the 519 nm band confirms the MMCT character of the 519 nm transition. The application of the Hush model[24] to the experimental MMCT band data (Table 2) gives α^2 and H_{if} values of 5.3 × 10^{-3} and 1383 cm^{-1} (**1**), and 5.6 × 10^{-3} and 1468 cm^{-1} (**2**). The determined α^2 and H_{if} values are consistent with those obtained for localised mixed-valence cyano bridged complexes $[(bpy)_2Cr(\mu\text{-}NC)_2M(CN)_6]^{-}$ (M = Mo, W),[25–28] but significantly higher than for $[(NH_3)_5Os(\mu\text{-}NC)M(CN)_7]^{-}$.[15,29–31]

The ν_{CN} region in the IR spectra reveals two broad bands at 2113(vvs) and 2150(vs) cm^{-1} for **1** and 2118(vvs) and 2150(vs) cm^{-1} for **2**. The bands of energy lower than 2140 cm^{-1} are characteristic of the terminal ν_{CN} in the isolated octacyanotungstate(IV) ion. The higher frequency band at 2150 cm^{-1} for **1** and **2** is assigned to bridging ν_{CN}, in agreement with the dominant kinematic effect, which results in constraints on the motion of CN^{-} and increase of ν_{CN}.[1b,d,e,g,i–k,11]

Kinetics

The self-assembly of the tetranuclear $\{[Co^{III}(N_4)]_2[W^{IV}(CN)_8]_2\}^{2-}$ square has been performed by employing two *cis*-$[Co(N_4)Cl_2]^{+}$ isomers, differing in reactivity. The completion of the reaction of *cis*-$[Co(trien)Cl(OH_2)]^{+}$ with $[W(CN)_8]^{4-}$ requires five hours, affording the $\{[Co^{III}(trien)]_2[W^{IV}(CN)_8]_2\}^{2-}$ square, which can be precipitated as soluble $K_2\{[Co^{III}(trien)]_2[W^{IV}(CN)_8]_2\}\cdot 8H_2O\cdot EtOH$ (**1**). The product of the reaction of *cis*-$[Co(tren)Cl_2]^{+}$ $K_2\{[Co^{III}(tren)]_2[W^{IV}(CN)_8]_2\cdot 9H_2O$ (**2**), however, starts to precipitate immediately. Formation of the $\{[Co^{III}(tren)]_2[W^{IV}(CN)_8]_2\}^{2-}$ tetranuclear square was confirmed by X-ray crystallography. The formation of the $\{[Co^{III}(trien)]_2[W^{IV}(CN)_8]_2\}^{2-}$ tetranuclear square was confirmed by identical electrochemical behaviour, identical spectra and spectroscopic characteristics of both $\{[Co^{III}(N_4)]_2[W^{IV}(CN)_8]_2\}^{2-}$ species. Moreover, the ESI MS strongly suggest the formation of $\{[Co^{III}(trien)]_2[W^{IV}(CN)_8]_2\}^{2-}$ square as the stable product.

The kinetics of the self-assembly of the $\{[Co^{III}(trien)]_2[W^{IV}(CN)_8]_2\}^{2-}$ unit was studied under pseudo-conditions with the excess of $[W(CN)_8]^{4-}$ over *cis*-$[Co(trien)Cl(OH_2)]^{2+}$ complex. The stoichiometry of formation of the $\{[Co^{III}(trien)]_2[W^{IV}(CN)_8]_2\}^{2-}$ [eqn. (1)] has been established by the Job method combined with a least-square fitting routine applied also to determine overall equilibrium constant β:

$$2cis\text{-}[Co(trien)(Cl)(OH_2)]^{2+} + 2[W(CN)_8]^{4-} \overset{\beta}{\rightleftharpoons} \{[Co(trien)]_2[W(CN)_8]\}^{2-} + 2Cl^{-} + 2H_2O \quad (1)$$

The Co : W = 2 : 2 stoichiometry of the product of the aggregation reaction conforms to the fundamental building square unit $\{[Co^{III}(trien)]_2[W^{IV}(CN)_8]_2\}^{2-}$. The relatively high log β value of 8.72 indicates that *cis*-$[Co(trien)Cl(OH_2)]^{2+}$ self-assembles with $[W(CN)_8]^{4-}$ giving a stable square unit structure. The kinetic data exhibit biphasic behaviour (Fig. 8). The least square fitting routine and application of kinetics modelling procedure included in the Specfit® software package[7] reveals that the reaction proceeds through two parallel pathways: second-order dependence in $[Co^{III}]$ pathway (k_{obs}^{I}) and first-order dependence in $[Co^{III}]$ pathway (k_{obs}^{II}) [eqn. (2)].

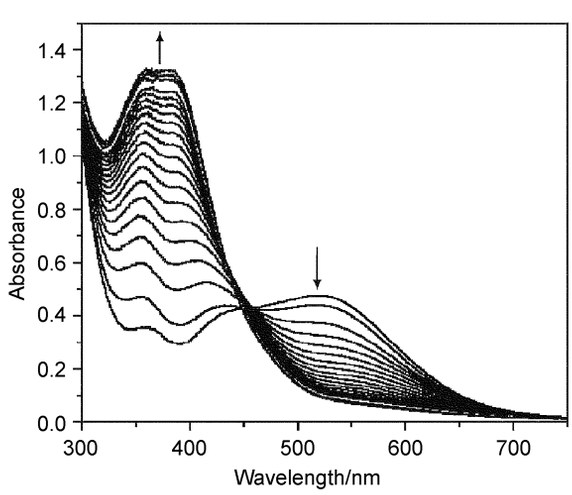

Fig. 7 The spectral changes during the oxidation of $\{[Co^{III}(trien)]_2[W^{IV}(CN)_8]_2\}^{2-}$ by saturated aqueous solution of $S_2O_8^{2-}$ (c_{tot} = 3.7 × 10^{-4} mol dm^{-3}). The arrows indicate the direction of changes. The time intervals between each spectrum were 120 s.

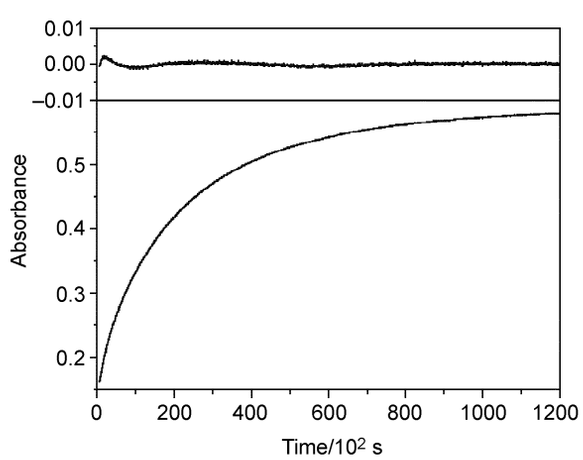

Fig. 8 Bottom: a typical plot of two-step kinetics of the substitution reaction *cis*-$[Co(trien)(OH_2)(Cl)]^{2+}$ by $[W(CN)_8]^{4-}$ ions. Top: the plot of difference between experimental and fitted curves, $[Co(trien)(OH_2)(Cl)]^{2+}$ = 1.0 × 10^{-3} mol dm^{-3}, $[W(CN)_8]^{4-}$ = 8.99 × 10^{-3} mol dm^{-3}, pH = 2, I = 0.5 mol dm^{-3} (buffer + KCl), T = 30 °C, λ = 550 nm.

Table 2 The experimental spectroscopic data and Hush parameters for MMCT transitions in $\{[Co^{III}(N_4)]_2[W^{IV}(CN)_8]_2\}^{2-}$

Compound	ν_{max}/cm^{-1}	ε_{max}/dm^3 mol^{-1} cm^{-1}	$\Delta\nu_{½}$, ($\Delta\nu_{½(calc)}$) [a]/cm^{-1}	d/Å	α^2 ($\alpha^2_{(calc)}$) [a]/10^3	H_{if}/cm^{-1}	Ref.
$\{[Co^{III}(trien)]_2[W^{IV}(CN)_8]_2\}^{2-}$	19 000	1 233	5 200 (6155)	5.18	5.3 (6.2)	1 383	this work
$\{[Co^{III}(tren)]_2[W^{IV}(CN)_8]_2\}^{2-}$	19 531	1 244	5617 (6214)	5.18	5.6 (6.2)	1 468	this work
$W^{IV}Cr^{III}$	17 794	2 160	5 890	5.3	15.9	2 248	23
$Mo^{IV}Cr^{III}$	19 417	3 040	6 000	5.3	10.2	1 963	23
$Mo^{IV}Os^{III}$	15 670	995	3 430	5.2	3.4 (5.8)	915	24
$W^{IV}Os^{III}$	13 945	1 460	3 340	5.2	5.5 (7.4)	1 030	24

[a] Values calculated from $\Delta\nu_{1/2} = [2300\ (\nu_{max} - \Delta E_o)]^{1/2}$, $\Delta E_o = 8064$, $\Delta E_{1/2}$[24] for $\Delta E_{1/2} = 0.34$ V.

$$\frac{d\{[Co(N_4)]_2[W(CN)_8]_2\}}{dt} = k_{obs}^{I}[Co(N_4)]^2 + k_{obs}^{II}[Co(N_4)] \quad (2)$$

The observed rate constants k_{obs} and k_{obs}^{II} show a linear dependence on the concentration of $[W(CN)_8]^{4-}$ (Figs. 9 and 10). The value of k_{obs}^{II} *vs.* $[W(CN)_8]^{4-}$ has the residual value at zero $[W(CN)_8]^{4-}$ (k_{-b}). The overall experimental rate equation therefore holds [eqn. (3)].

$$\frac{d\{[Co(N_4)]_2[W(CN)_8]_2\}}{dt} = k_a[Co(N_4)]^2\ [W(CN)_8] + k_b[Co(N_4)]\ [W(CN)_8] + k_{-b}[Co(N_4)] \quad (3)$$

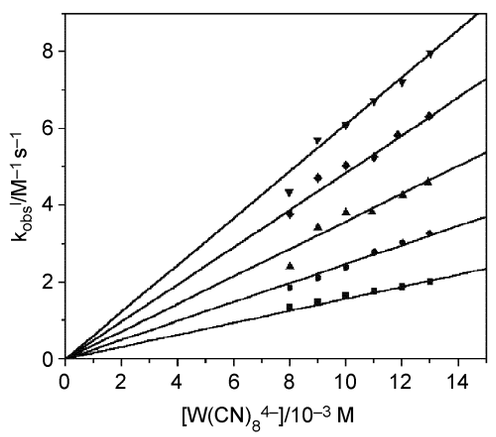

Fig. 9 The plot of k_{obs}^{I} *versus* $[W(CN)_8]^{4-}$ at 10 (■), 15 (●), 20 (▲), 25 (◆) and 30 °C (▼); $[Co(trien)(OH_2)(Cl)]^{2+} = 1.0 \times 10^{-3}$ mol dm^{-3}, pH = 2, $I = 0.5$ mol dm^{-3} (buffer + KCl).

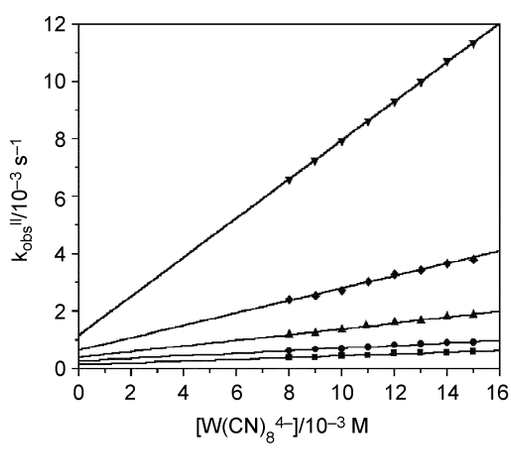

Fig. 10 The plot of k_{obs}^{II} *versus* $[W(CN)_8]^{4-}$ at 10 (■), 15 (●), 20 (▲), 25 (◆) and 30 °C (▼); $[Co(trien)(OH_2)(Cl)]^{2+} = 1.0 \times 10^{-3}$ mol dm^{-3}, pH = 2, $I = 0.5$ mol dm^{-3} (buffer + KCl).

The rate constants k_a, k_b, k_{-b} and the activation parameters $\Delta H^{\neq}$, $\Delta S^{\neq}$ derived from temperature dependence of the appropriate rate constants are: $k_a = 4.89 \times 10^2$ dm^6 mol^{-2} s^{-1}, $\Delta H^{\neq} = 46$ kJ mol^{-1}, $\Delta S^{\neq} = -38$ J K^{-1} mol^{-1}; $k_b = 2.14 \times 10^{-1}$ dm^3 mol^{-1} s^{-1}, $\Delta H^{\neq} = 121$ kJ mol^{-1}, $\Delta S^{\neq} = +149$ J K^{-1} mol^{-1}; $k_{-b} = 0.66 \times 10^{-3}$ dm^3 mol^{-1} s^{-1}, $\Delta H^{\neq} = 68$ kJ mol^{-1}, $\Delta S^{\neq} = -77$ J K^{-1} mol^{-1}($T = 25$ °C, pH = 2 (HCl + KCl), $I = 0.5$ mol dm^{-3}). The detailed kinetic data are included in Table S2.† On the basis of the observed kinetics, we propose the following mechanism of the self-assembly of *cis*-$[Co(trien)Cl(OH_2)]^{2+}$ with $[W(CN)_8]^{4-}$ leading to the formation of $\{[Co(trien)]_2[W(CN)_8]_2\}^{2-}$ square (Scheme 1) where 'et' indicates electron transfer step and gives an overall rate equation [eqn. (4)] consistent with the experimental one,

$$\frac{d\{[Co(N_4)]_2[W(CN)_8]_2\}}{dt} = k_1K_{IP}K_{ITr}[Co(N_4)]^2\ [W(CN)_8] + k_2K_{IP}[Co(N_4)]\ [W(CN)_8] + k_{-2}[Co(N_4)] \quad (4)$$

where $k_1K_{IP}K_{ITr} = k_a$, $k_2K_{IP} = k_b$ and $k_{-2} = k_{-b}$.

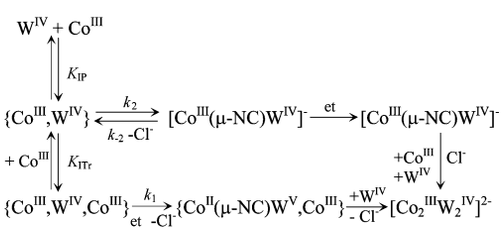

Scheme 1

The reaction consists of two parallel reaction pathways preceded by the formation of the $\{[Co^{III}(trien)Cl(OH_2)]^{2+}, [W^{IV}(CN)_8]^{4-}\}$ ion pair (hereafter named $\{Co^{III},W^{IV}\}$) between *cis*-$[Co(trien)Cl(OH_2)]^{2+}$ and $[W(CN)_8]^{4-}$. The value of the ion pair formation constant K_{IP} can be estimated on the basis of the Eigen–Fuoss expressions.[32] The model of the hydrogen bonded ion-pair with the distance of 8.1 Å between the metal centres gives the value of K_{IP} of 7 dm^3 mol^{-1}.

The second-order dependence in $[Co^{III}]$ pathway (k_a) can be explained in terms of the formation of the ion triplet $\{[Co^{III}(trien)Cl(OH_2)]^{2+}, [W^{IV}(CN)_8]^{4-}, [Co^{III}(trien)Cl(OH_2)]^{2+}\}$, favoured by its electroneutrality, which undergoes an outer-sphere electron transfer (OSET) rate-determining step followed by the formation of trinuclear $\{Co^{II}(\mu\text{-}NC)W^{V},Co^{III}\}$ transient species. The labile $\{Co^{II}(\mu\text{-}NC)W^{V},Co^{III}\}$ transient species undergoes fast substitution by $[W^{IV}(CN)_8]^{4-}$ and spontaneous back electron transfer to generate the tetranuclear $\{[Co^{III}(trien)]_2[W^{IV}(CN)_8]_2\}^{2-}$ product. The OSET rate-determining step is in agreement with the well known mechanism for the formation of cyano-bridged compounds between Co^{III} and cyanometallates.[29,33–39] The second-order pathway conforms to the second-order reduction of trisoxalatocobaltate(III) by iron(II),[39] where the formation of trinuclear transient species has been rationalised in terms of additional transient intermediate stabilisation by the delocalisation of the electron between both Co centres. The negative activation entropy has been found in majority of OSET reactions of Co^{III} compounds and octacyanometallates.[33,37a,40,41]

The first-order dependence in [Co^{III}] pathway (k_b, k_{-b}) can be explained assuming the reversible formation of cyano-bridged {[(trien)$(OH_2)Co^{III}$(μ-NC)$W^{IV}(CN)_7$]}$^-$ dinuclear complex, followed by inner-sphere electron transfer (ISET) process.[30,40,42,43] The {Co^{II}(μ-NC)W^V} dinuclear labile transient species may undergo subsequent fast aggregation and spontaneous back electron transfer producing stable tetranuclear {[Co^{III}(trien)]$_2$-[$W^{IV}(CN)_8]_2$}$^{2-}$ square. The substitutionally controlled inner-sphere electron transfer mechanism is supported by the large and positive activation entropy for the forward step (k_b), which is commonly observed for substitution reactions of low spin Co^{III} complexes.[40,41b,42,43] However, the activation entropy values are influenced by charge changes which make them less distinctive. Thus, the possibility of reversible outer-sphere reaction of first-order dependence in [Co^{III}] pathway (k_b, k_{-b}) cannot be ruled out.[34] The studies of redox kinetics of the Co^{III} complexes have demonstrated that electron transfer reactions involving bridging ligands can follow both, outer- and inner-sphere mechanisms, simultaneously.[40,42]

The reaction kinetics was studied in the pH range of 2–9. The reaction significantly decelerates with increasing pH. Therefore pH dependence over the range of pH 2–9 could be resolved only for the second order dependence in the Co^{III} pathway (k_a). The pH dependence of k_a as a function of pH is shown in Fig. 11. The S-shape profile of the k_a *vs.* pH strongly suggests that *cis*-[Co(trien)$Cl(OH_2)]^{2+}$ is involved in an acid–base equilibrium in the pH range investigated. The limiting rate constants at the higher and lower acidities correspond to the acidic and basic forms of the Co^{III} precursor, eqn. (5). The rate law associated with this system is given by eqn. (6), where k_a is the

$$cis\text{-}[Co(trien)Cl(OH_2)]^{2+} \rightleftharpoons cis\text{-}[Co(trien)Cl(OH)] + H^+ \quad (5)$$

$$k_a = \frac{k_p[H^+]}{[H^+] + K_a}[W(CN)_8] \quad (6)$$

acid dissociation constant of *cis*-[Co(trien)$Cl(OH_2)]^{2+}$ and k_p is its rate constant. The values of pK_a and k_p are 5.8 and 156 ± 12 M^{-2} s^{-1}, respectively (T = 25 °C; I = 0.5 M; [Co(trien)] : [$W(CN)_8$] = 1 : 10). The value of pK_a = 5.8 is in a good agreement with pK_a = 5.9 (T = 20 °C; I = 0.1 M) derived from titration of *cis*-[Co(trien)$Cl(OH_2)]^{2+}$ in aqueous solution.[3]

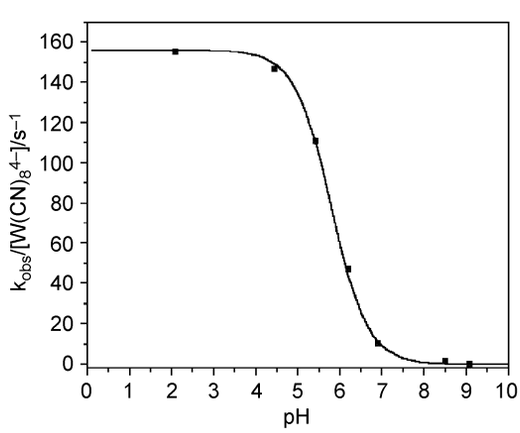

Fig. 11 The plot of $k_{obs}^{I}/[W(CN)_8]^{4-}$ *versus* pH at 25 °C, [Co(trien)-$(OH_2)(Cl)]^{2+}$ = 1.0 × 10^{-3} mol dm^{-3}, $[W(CN)_8]^{4-}$ = 1.0 × 10^{-2} mol dm^{-3}, I = 0.5 mol dm^{-3} (buffer + KCl).

Conclusion

We succeeded in the synthesis of two novel octacyanotungstate(IV) supramolecular assemblies: K_2[Co^{III}(tren)]$_2$-[$W^{IV}(CN)_8]_2$· $9H_2O$ (**1**) and K_2[Co^{III}(trien)]$_2$[$W^{IV}(CN)_8]_2$·$8H_2O$· EtOH (**2**), and crystallographic characterisation of **1**. The Co(III) and W(IV) centres are linked alternatively by single cyano bridge affording {[Co(tren)]$_2$[$W(CN)_8]_2$}$^{2-}$ square units joined by potassium ions into the 2D bi-layers. A mechanistic pathway has been presented to explain the self-assembly of $[W(CN)_8]^{4-}$ and *cis*-[Co^{III}(trien)$Cl(OH_2)]^{2+}$ into {[Co(trien)]$_2$-[$W(CN)_8]_2$}$^{2-}$. The reaction proceeds through two parallel pathways involving formation of an ion-pair {[Co^{III}(trien)-$Cl(OH_2)]^{2+}$, $[W^{IV}(CN)_8]^{4-}$} and ion-triplet {[Co^{III}(trien)-$Cl(OH_2)]^{2+}$, $[W^{IV}(CN)_8]^{4-}$, [Co^{III}(trien)$Cl(OH_2)]^{2+}$}. The ion-triplet undergoes a rate-determining outer-sphere electron-transfer step ($W^{IV} \longrightarrow Co^{III}$) followed by fast aggregation due to a labile Co^{II} centre being formed and spontaneous back electron-transfer to generate the {[Co^{III}(trien)]$_2$[$W^{IV}(CN)_8]_2$}$^{2-}$ product. The ion-pair undergoes rate-determining reversible substitution of Cl^- ligand creating cyano-bridged intermediate {[(trien)(OH_2)Co(μ-NC)$W(CN)_8]_2$}$^-$ and a further inner-sphere electron transfer step ($W^{IV} \longrightarrow Co^{III}$). The {[(trien)$(OH_2)Co^{II}$-(μ-NC)$W^V(CN)_8]_2$}$^-$ intermediate species undergoes fast aggregation and spontaneous back electron-transfer to generate the tetranuclear product.The {[$Co(N_4)]_2$[$W(CN)_8]_2$}$^{2-}$ tetranuclear square exhibits MMCT transitions at 519 nm (**1**) and 512 nm (**2**). The mixed-valence features make them very promising candidates for photomagnetic systems. Further work along line is currently in progress.

Acknowledgements

Dr Piotr Suder is thanked for the helpful discussion of ESI MS spectra.

References

1 (*a*) J. Lu, W. T. A. Harrison and A. J. Jacobson, *Angew. Chem., Int. Ed. Engl.*, 1995, **34**, 2557; (*b*) B. Sieklucka, J. Szklarzewicz, T. J. Kemp and W. Errington, *Inorg. Chem.*, 2000, **34**, 2557; (*c*) Z. J. Zhong, H. Seino, Y. Mizobe, M. Hidai, A. FujiShima, S. Ohkoshi and K. Hashimoto, *J. Am. Chem. Soc.*, 2000, **122**, 2952; (*d*) Z. J. Zhong, H. Seino, Y. Mizobe, M. Hidai, M. Verdaguer, S. Ohkoshi and K. Hashimoto, *Inorg. Chem.*, 2000, **39**, 5095; (*e*) A. K. Sra, G. Rombaut, F. Lahitête, S. Golhen, L. Ouahab, C. Mathonière, J. V. Yakhmi and O. Kahn, *New J. Chem.*, 2000, **24**, 871; (*f*) G. Rombaut, S. Golhen, L. Ouahab, C. Mathonière and O. Kahn, *J. Chem. Soc., Dalton Trans.*, 2000, 3609; (*g*) R. Podgajny, Y. Dromzée, K. Kruczala and B. Sieklucka, *Polyhedron*, 2001, **20**, 685; (*h*) S. Ohkoshi and K. Hashimoto, *J. Photochem. Photobiol. C: Photochem. Rev.*, 2001, **2**, 71; (*i*) G. Rombaut, M. Verelst, S. Golhen, L. Ouahab, C. Mathonière and O. Kahn, *Inorg. Chem.*, 2001, **40**, 1151; (*j*) G. Rombaut, C. Mathonière, P. Guionneau, S. Golhen, L. Ouahab, M. Verelst and P. Lecante, *Inorg. Chim. Acta*, 2001, **326**, 27; (*k*) R. Podgajny, C. Desplanches, B. Sieklucka, R. Sessoli, V. Villar, C. Paulsen, W. Wernsdorfer, Y. Dromzee and M. Verdauger, *Inorg. Chem.*, 2002, **41**, 1323; (*l*) D-F. Li, S. Gao, L-M. Zheng, W-Y. Sun, T. Okamura, N. Ueyama and W-X. Tang, *New J. Chem.*, 2002, **4**, 485.
2 F. Basolo, *J. Am. Chem. Soc.*, 1948, **70**, 2634.
3 (*a*) A. M. Sargeson and G. H. Searle, *Inorg. Chem.*, 1967, **6**, 787; (*b*) A. M. Sargeson and G. H. Searle, *Inorg. Chem.*, 1967, **6**, 2173.
4 J. G. Leipold, L. D. C. Bok and P. J. Cilliers, *Z. Anorg. Allg. Chem.*, 1974, **409**, 343.
5 T. P. Dasgupta and G. M. Harris, *J. Am. Chem. Soc.*, 1975, **97**, 1733.
6 J. Lusie, *Handbook of Analytical Chemistry*, Mir, Moscow, 1975, p. 263.
7 *Specfit* provided by R. A. Binstead, Spectrum Software Associates, Chapel Hill, NC.
8 Z. Otwinowski and W. Minor, *Methods Enzymol.*, 1997, **276**, 307.
9 G. M. Sheldrick, SHELX-97, Programs for structure analysis, University of Göttingen, Germany, 1998.
10 M. N. Burnett and C. K. Johnson, ORTEP-III: Oak Ridge Thermal Ellipsoid Plot Program for Crystal Structure Illustrations, Report ORNL-6895, Oak Ridge National Laboratory, Oak Ridge, TN, USA, 1996.
11 J. G. Leipold, L. D. C. Bok and S. S. Besson, *Acta Crystallogr., Sect. B*, 1970, **26**, 684.
12 (*a*) R. L. Fanshawe and A. G. Blackmann, *Inorg. Chem.*, 1995, **34**, 421; (*b*) R. L. Fanshawe, A. Mobinikhaledi, C. R. Clark and A. G. Blacman, *Inorg. Chim. Acta*, 2000, **307**, 26.

13 A. Yuan, J. Zou, B. Li, Z. Zha, C. Duan, Y. Liu, Z. Xu and S. Keizer, *Chem. Commun.*, 2000, 1297.
14 E. Colacio, J. M. Domínguez-Vera, M. Ghazi, R. Kivekäs, J. M. Moreno and A. Pajunen, *J. Chem. Soc., Dalton Trans.*, 1999, 505.
15 (*a*) P. V. Bernhardt, B. P. Macpherson and M. Martinez, *Inorg. Chem.*, 2000, **39**, 5203; (*b*) P. V. Bernhardt, B. P. Macpherson and M. Martinez, *J. Chem. Soc., Dalton Trans.*, 2002, 1435.
16 Z. N. Chen, R. Appelt and H. Vahrenkamp, *Inorg. Chim. Acta*, 2000, **309**, 65.
17 P. V. Bernhardt and M. Martinez, *Inorg. Chem.*, 1999, **38**, 424.
18 D. H. Vaughan, Electrochemical Properties in Aqueous Solutions, and Ch. J. Pickett, Electrochemical Properties in Non-aqueous Solutions, in *Comprehensive Coordination Chemistry*, Pergamon, Oxford, 1987, vol. 1, ch. 8.2 and 8.3, pp. 479–501.
19 A. Vogler and H. Kunkely, *Ber. Bunsen-Ges. Phys. Chem.*, 1975, **79**, 83.
20 (*a*) R. A. Costelló, C. P. Mac-Coll, N. B. Egen and A. Haim, *Inorg. Chem.*, 1969, **8**, 699; (*b*) R. A. Costelló, C. P. Mac-Coll and A. Haim, *Inorg. Chem.*, 1971, **10**, 203.
21 (*a*) A. Golebiewski and H. Kowalski, *Theor. Chim. Acta*, 1968, **12**, 293; (*b*) A. Golebiewski and R. Nalewajski, *Z. Naturforsch., A*, 1972, **27**, 1672.
22 (*a*) E. A. Almaraz, L. A. Gentil, L. M. Brando and J. A. Olabe, *Inorg. Chem.*, 1996, **35**, 7718; (*b*) G. A. Neyhart, C. J. Timpson, W. D. Bates and T. J. Meyer, *J. Am. Chem. Soc.*, 1996, **118**, 3730; (*c*) R. Podgajny, B. Sieklucka and W. Lasocha, *J. Chem. Soc., Dalton Trans.*, 2000, 1799; (*d*) B. Sieklucka, W. Lasocha, L. M. Proniewicz, R. Podgajny and H. Schenk, *J. Mol. Struc.*, 2000, **520**, 150.
23 (*a*) W. C. Jones and W. E. Bull, *J. Chem. Soc. A*, 1968, 1849; (*b*) M. C-L. Yang and R. A. Palmer, *J. Am. Chem. Soc.*, 1975, **97**, 5390.
24 N. S. Hush, *Prog. Inorg. Chem.*, 1967, **8**, 391.
25 B. M. Pfenning, V. A. Fritchman and K. A. Hayman, *Inorg. Chem.*, 2001, **40**, 255.
26 K. D. Demadis, C. M. Hartshorn and T. J. Meyer, *Chem. Rev.*, 2001, **101**, 2655.
27 Rafal Kania and B. Sieklucka, *Polyhedron*, 2000, **19**, 2225.
28 B. W. Pfennig, A. B. Bocarsly and R. K. Prud'homme, *J. Am. Chem. Soc.*, 1993, **115**, 2661.
29 M. Laidlow and R. G. Denning, *Inorg. Chim. Acta*, 1994, **219**, 121.
30 A. P. Szecsy and A. Haim, *J. Am. Chem. Soc.*, 1981, **103**, 1679.
31 R. Billing and A. Vogler, *J. Photochem. Photobiol. A: Chem.*, 1997, **103**, 239.
32 (*a*) R. M. Fuoss, *J. Am. Chem. Soc.*, 1958, **80**, 5059; (*b*) M. Eigen, *Z. Phys. Chem.*, 1954, **1**, 176.
33 M. Martinez, M-A. Pitarque and R. van Eldik, *Inorg. Chim. Acta*, 1997, **256**, 51.
34 M. Galán, M. M. Graciani, R. Jiménez, M. L. Moyá, E. Muñoz, A. Rodriguez and F. Sánchez, *Ber. Bunsen-Ges. Phys. Chem.*, 1996, **100**, 470.
35 A. D. Jordan, S. L. Scott and R. D. Jordan, *Inorg. Chim. Acta*, 1995, **239**, 99.
36 P. Martinez, J. Zuluaga, P. Noheda and R. van Eldik, *Inorg. Chim. Acta*, 1992, **195**, 249.
37 (*a*) R. van Eldik and H. Kelm, *Inorg. Chim. Acta*, 1983, **73**, 91; (*b*) I. Krack and R. van Eldik, *Inorg. Chem.*, 1986, **25**, 1743; (*c*) I. Krack and R. van Eldik, *Inorg. Chem.*, 1989, **28**, 851; (*d*) I. Krack and R. van Eldik, *Inorg. Chem.*, 1990, **29**, 1700.
38 P. L. Gaus and J. L. Villanueva, *J. Am. Chem. Soc.*, 1980, **102**, 1934.
39 R. D. Cannon and J. S. Stillman, *J. Chem. Soc., Dalton Trans.*, 1976, 428.
40 R. G. Wilkins, *Kinetics and Mechanism of Reactions of Transition Metal Complexes*, VCH, Weinheim, 2nd edn., 1991, ch. 4.3, 5.3 and 5.7, pp. 212–219, 259–276; and references therein.
41 (*a*) G. F. McKnight and G. P. Haight, *Inorg. Chem.*, 1973, **12**, 1619; (*b*) J. G. Leipoldt, S. S. Basson, G. J. Lamprecht and D. R. Rabie, *Inorg. Chim. Acta*, 1981, **51**, 67; (*c*) K. W. Hicks and M. A. Hurless, *Inorg. Chim. Acta*, 1983, **74**, 229.
42 (*a*) H. Taube, H. Meyers and L. R. Rich, *J. Am. Chem. Soc.*, 1953, **75**, 4118; (*b*) H. Taube and H. Meyers, *J. Am. Chem. Soc.*, 1954, **76**, 2103; (*c*) L. Rosenhein, D. Speiser and A. Haim, *Inorg. Chem.*, 1974, **13**, 1571; (*d*) J. Phillips and A. Haim, *Inorg. Chem.*, 1980, **19**, 1616; (*e*) K. Bernauer, D. Hugi-Cleary, H. J. Hilgers, H. Abd-el-Khalek, N. Brügger and C. Kressl, *Inorg. Chim. Acta*, 1998, **275–276**, 1; (*f*) H. J. Hilgers and K. Bernauer, *Inorg. Chim. Acta*, 1998, **275–276**, 9.
43 (*a*) M. S. A. Hamza, C. Dücker-Benfer and R. van Eldik, *Inorg. Chem.*, 2000, **39**, 3777; (*b*) M. S. A. Hamza, X. Zou, K. L. Brown and R. van Eldik, *Inorg. Chem.*, 2001, **40**, 5440; (*c*) Z-L. Lu, M. S. A. Hamaza and R. van Eldik, *Eur. J. Inorg. Chem.*, 2001, 503.